Thermal transport of the single-crystal rare-earth nickel borocarbides $R\mathrm{Ni_2B_2C}$

B. D. Hennings* and D. G. Naugle†
Physics Department, Texas A&M University, College Station, Texas 77843-4242

P. C. Canfield
Department of Physics & Astronomy, Iowa State University, Ames, Iowa 50011
(Received 22 August 2002; published 12 December 2002)

The quaternary intermetallic rare-earth nickel borocarbides $R\mathrm{Ni_2B_2C}$ are a family of compounds that show magnetic behavior, superconducting behavior, and/or both. Thermal transport measurements reveal both electron and phonon scattering mechanisms, and can provide information on the interplay of these two long-range phenomena. In general the thermal conductivity κ is dominated by electrons, and the high temperature thermal conductivity is approximately linear in temperature and anomalous. For $R=$Tm, Ho, and Dy the low-temperature thermal conductivity exhibits a marked loss of scattering at the antiferromagnetic ordering temperature T_N. Magnon heat conduction is suggested for $R=$Tm. The κ data for $R=$Ho lends evidence for gapless superconductivity in this material above T_N. Unlike the case for the non-magnetic superconductors in the family, $R=$Y and Lu, a phonon peak in the thermal conductivity below T_c is not observed down to $T=1.4$ K for the magnetic superconductors. Single-crystal quality seems to have a strong effect on κ. The electron-phonon interaction appears to weaken as one progresses from $R=$Lu to $R=$Gd. The resistivity data shows the loss of scattering at T_N for $R=$Dy, Tb, and Gd; and the thermoelectric power for all three of these materials exhibits an enhancement below T_N.

DOI: 10.1103/PhysRevB.66.214512 PACS number(s): 74.70.Dd, 75.50.Ee, 74.25.Fy

I. INTRODUCTION

Thermal conductivity is a very useful tool in the investigation of electron-phonon interaction, particularly in the superconducting state where many other transport properties provide little or no information. Recently discovered quaternary intermetallic compounds $R\mathrm{Ni_2B_2C}$ (where $R=$a rare earth or Y) have attracted much attention because of the rich variety of magnetic, superconducting, and heavy fermion phenomena exhibited by them. $\mathrm{YNi_2B_2C}$ and $\mathrm{LuNi_2B_2C}$ are nonmagnetic superconductors; whereas $\mathrm{TbNi_2B_2C}$ and $\mathrm{GdNi_2B_2C}$ exhibit magnetic order but not superconductivity. However, for the compounds of the rare-earth elements Dy, Er, Ho and Tm, superconductivity and magnetic order coexist (see Naugle *et al.*[1] for a recent review).

To obtain a better understanding of the electron-phonon interaction, the a–b plane thermal conductivity κ, absolute thermopower S, and electrical resistivity ρ were measured on the same single-crystal sample for each $R\mathrm{Ni_2B_2C}$ compound, where $R=$Y, Lu, Yb, Tm, Er, Ho, Dy, Tb, and Gd. The resistivity and thermo-electric power have been previously measured for this family of materials by others. However, due to the sensitive dependence of $\rho(T)$ and $S(T)$ on the stoichiometry and the single-crystal quality and purity, it is essential to measure $\rho(T)$ and $S(T)$ on these samples for a characterization of the sample and an interpretation of the thermal conductivity data. The results for all of these materials are reported here with the exception of the heavy fermion compound $R=$Yb. Two samples of $\mathrm{ErNi_2B_2C}$ grown at different times have been measured. The data for both samples are discussed, but not all of the data for both of the $\mathrm{ErNi_2B_2C}$ samples are shown in this paper. All samples were provided by Ames Laboratory and were grown by the $\mathrm{Ni_2B}$ flux method discussed by Xu *et al.*[2] With the exception of $\mathrm{ErNi_2B_2C}$, the samples are single-phase, reasonably high-quality single crystals. The preceding statement is based on the residual resistivity ratios, the residual resistivity, the sharpness and completeness of the superconducting transition, and the temperatures of the superconducting and magnetic transitions.

II. EXPERIMENTAL DETAILS

The four-terminal resistance was measured separately from κ and S, which were measured at the same time. The thermal conductivity was measured by the steady-state linear heat flow method. One end of the sample was thermally isolated, a known, constant heat input via a resistive heater was applied to that end, and the resultant steady state temperature gradient was measured. The temperature difference between the two ends of the sample was measured with a Au-Fe-chromel thermocouple. Verification of the temperature difference was provided by a chromel-constantan thermocouple for most of the temperature range. The sample was completely surrounded by a thermal shield held at the temperature of the cold end. Even though heat leaks were minimized by design, the actual heat leaks were measured and accounted for in the thermal conductivity data. Thermal conductivity measurements for a high-purity, well-annealed Ag foil agreed within an experimental uncertainty of accepted values. The thermoelectric power measurements were calibrated by measuring a well-annealed piece of pure lead foil and comparing the results to the accepted standard lead thermoelectric power reported by Roberts.[3] The greatest source of error in the thermal conductivity and resistivity data is due to inaccuracies in the determination of the sample dimensions. Sample dimensions for all samples were determined by using a Gaertner optical comparator. A detailed discussion

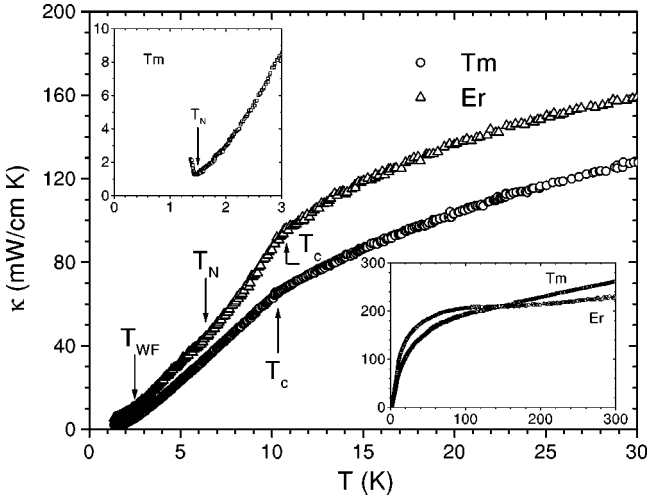

FIG. 1. κ(mW/cm-K) vs $T(K)$ for $TmNi_2B_2C$–○ and $ErNi_2B_2C$ sample number 2–△ over several temperature ranges. Arrows show superconducting and magnetic transitions.

of the experimental techniques can be found in the paper by Hennings.[4]

III. RESULTS AND DISCUSSION

A. κ of $TmNi_2B_2C$ and $ErNi_2B_2C$

The inset in the lower right of Fig. 1 depicts the *a*-*b* plane κ of $TmNi_2B_2C$, and the $ErNi_2B_2C$ number two sample plotted versus temperature from 1.5 to 300 K. The high-temperature κ's for both materials (all three samples) are approximately linear in temperature and similar in magnitude. Using a Wiedemann-Franz analysis with the measured ρ for these samples, the κ for all three samples ($TmNi_2B_2C$ and both $ErNi_2B_2C$) is dominated by the electronic portion κ_e at T_c, while at 300 K, κ_e for all three samples is only about one-half of the total measured κ.

Typically, metalliclike samples exhibit a distinct peak in the thermal conductivity, usually around $(0.1–0.3)\Theta_D$, where Θ_D is the Debye temperature. Electrons appear to be responsible for one-half or more of the thermal conduction for the entire temperature range from T_c to 300 K in these two materials. Additionally, S and ρ for these two materials are metallic in nature, as discussed later in this paper. It is therefore interesting that there is no sign of a phonon or electron peak in the high-temperature thermal conductivity for $TmNi_2B_2C$ or either $ErNi_2B_2C$ sample well past the temperature of the ordinary peak, $(0.1–0.3)\Theta_D$. The Debye temperature is estimated as ~348–353 K for $TmNi_2B_2C$ and ~349–354 K for $ErNi_2B_2C$ by a scaling of molar masses from $LuNi_2B_2C$. The Debye temperature for $LuNi_2B_2C$ was reported as ~350 K by Carter *et al.*[5] or ~345 K by Kim *et al.*[6]

Figure 1 depicts an expanded plot of the *a*-*b* plane κ of $TmNi_2B_2C$ and $ErNi_2B_2C$ sample number two plotted versus temperature from 1.5 to 30 K. The superconducting phase transitions ($T_c \simeq 11$ K for both $TmNi_2B_2C$ and $ErNi_2B_2C$) are clearly indicated in κ as a distinct change in slope as expected for a second-order phase transition.

A sharp increase in the low temperature thermal conductivity is readily seen for $TmNi_2B_2C$ in the upper left inset of Fig. 1 at about 1.4 K, very near $T_N = 1.5$ K. One possible explanation for this is that this increase could be accounted for by the loss of spin-flip scattering of electrons when the magnetic moments of the trivalent rare-earth ions, Tm^{3+}, in the sample change from the randomly oriented paramagnetic state to the ordered antiferromagnetic state. Due the fact that this increase in κ occurs at such a low temperature, approximately one-eighth of T_c, where the conduction electrons are expected to be mostly condensed, one of two explanations is required so electrons can be responsible for this sharp increase in κ. One possibility would be that in $TmNi_2B_2C$ the electrons responsible for thermal transport (possibly those that are also responsible for magnetic ordering of the rare-earth ions) are different from those participating in the Cooper pairs of superconductivity, i.e., a two-band model. A second explanation for how electrons could be responsible for this sharp increase in κ is gapless superconductivity. The upper critical field H_{c2}, does decrease by almost 3 kOe at T_N, as discussed in the review by Naugle *et al.*,[1] but it does not vanish. H_{c2} is also highly anisotropic.

A second possible cause of this increase in κ is the opening of a thermal conduction channel, namely that of magnetic spin waves better known as magnons. This would explain why the increase is relatively sharp since the magnons could appear suddenly at the onset of antiferromagnetic order, T_N. This is the most likely explanation.

A third possible explanation would be that the increase in thermal conduction is due to the lattice conduction increasing either due to loss of scattering from the random magnetic spins as they order, or due to increased conduction resulting from some lattice ''tuning'' at T_N. The lattice component is unlikely to be the cause of the increase since the thermal conduction more than doubles at $T = 1.4$ K, and the phonon conduction decreases as T^3 at low temperatures. Additionally, the phonon-magnetic moment interaction, and hence phonon-magnetic moment scattering, has been shown to be weak in this family of compounds by analyzing the behavior of the electrical resistivity and thermal conductivity for R = Dy, Tb, and Gd at T_N.[4] That is to say the increase in the total measured thermal conductivity at T_N was totally accounted for by the increase in κ_e, where κ_e was determined from the measured electrical resistivity and the Wiedemann-Franz law. The lattice ''tuning'' is also unlikely. It is possible that a lattice constant changes at T_N due to the magnetic phase transition. It is very unlikely that this dominant phonon mode is heavily populated due to the low temperatures ($T \leqslant 1.4$ K). Phonons are the least likely explanation for this sharp increase.

The data of Fig. 1 for $ErNi_2B_2C$ sample number two indicate a subtle increase in κ at $T_N = 6.8$ K due to the antiferromagnetic ordering of the magnetic moments of the Er^{3+} ions. The κ data for $ErNi_2B_2C$ sample number one do not indicate any change at T_N. Also, the low temperature κ data do not indicate any change at $T_{WF} = 2.3$ K due to the weak ferromagnetic ordering of the magnetic moments of the Er^{3+} ions for either of the $ErNi_2B_2C$ samples. The absence of an

indication of T_{WF} in the κ data is not alarming in the sense that the other sample of this family with weak ferromagnetic order, $TbNi_2B_2C$ (discussed later in this paper), does not exhibit any indication of T_{WF} in the κ data either.

One possible explanation of the absence of a larger/sharper indication of T_N in the κ data of both $ErNi_2B_2C$ samples would be that the anti-ferromagnetic ordering of the magnetic moments mainly affects the electron scattering and has a negligible impact on the phonon scattering. Since T_N is a little over one-half of T_c for $ErNi_2B_2C$, the majority of the electrons could already be condensed into Cooper pairs at this temperature; hence, the thermal conduction due to electrons should be small, and therefore the change in scattering of electrons at T_N could have a negligible affect on thermal conduction. In support of this argument is the fact that the change of the thermal conduction due to antiferromagnetic ordering is entirely accounted for by the change to electron thermal conduction for the $DyNi_2B_2C$, $TbNi_2B_2C$, and $GdNi_2B_2C$ samples, i.e., paramagnetic to antiferromagnetic ordering has minimal to no impact on lattice thermal conduction in these samples. This interpretation is based on the measured electrical resistivity and assumes that the Wiedemann-Franz law is valid near T_c.

Evidence against this argument is the fact that the upper critical field H_{c2} again decreases by almost 3 kOe at T_N (see Naugle *et al.*[1]), implying a shorter coherence length, fewer Cooper pairs, and more uncondensed electrons. H_{c2} is again highly anisotropic. The decrease in H_{c2} could alternatively be due to an increase in the internal magnetic field B_{int}, which could imply a higher superconducting electron density rather than a lower one.

A second possible explanation of the absence of a larger/sharper indication of T_N in the κ data of both $ErNi_2B_2C$ samples would be the lower quality of the $ErNi_2B_2C$ samples which is discussed later. The $ErNi_2B_2C$ sample number two appears to be higher quality than the $ErNi_2B_2C$ sample number one, but it is likely not as high a quality single crystal as the other members of the RNi_2B_2C family investigated here. The absence of an indication of T_N in the $ErNi_2B_2C$ number one sample κ data is attributed to the lower quality single crystal, and the likely presence of an unwanted (non-1221) phase or an unwanted contaminant.

Thermal conductivity data for temperatures below 25 K have been previously reported by Cao *et al.*[7] for a polycrystalline sample of each $TmNi_2B_2C$ and $ErNi_2B_2C$. The data reported in this paper are about 38% greater in magnitude for $TmNi_2B_2C$ and 400% greater for $ErNi_2B_2C$ than that reported by Cao *et al.* Additionally, the data of Cao *et al.* did not show a clear indication of T_c for $TmNi_2B_2C$, but did show an indication of both T_c and T_N for $ErNi_2B_2C$, with the T_N indication disappearing in non-zero external magnetic fields.

B. κ of $HoNi_2B_2C$ and $DyNi_2B_2C$

The inset of Fig. 2 depicts the $a-b$ plane κ of $HoNi_2B_2C$ and $DyNi_2B_2C$ plotted versus temperature from 1.5 to 300 K. The high temperature κ for both materials is again approximately linear in temperature and almost the same in magnitude. Using a Wiedemann-Franz analysis with the measured ρ for these two samples, the κ for both materials is dominated by the electronic portion κ_e at T_c, while at 300 K, κ_e for both samples is just above one-half of the total measured κ. Again electrons appear to be responsible for one-half or more of the thermal conduction for the entire temperature range from T_c to 300 K in these two materials. S and ρ for these two materials are also metallic in nature as discussed later in this paper. Again it is noteworthy that there is no sign of a phonon or electron peak in the high temperature thermal conductivity for either $HoNi_2B_2C$ or $DyNi_2B_2$ well past the temperature of the ordinary peak, $(0.1–0.3)\Theta_D$. The Debye temperature is estimated as $\sim 350–356$ K for $HoNi_2B_2C$ and $\sim 352–357$ K for $DyNi_2B_2C$ by scaling of molar masses from $LuNi_2B_2C$.

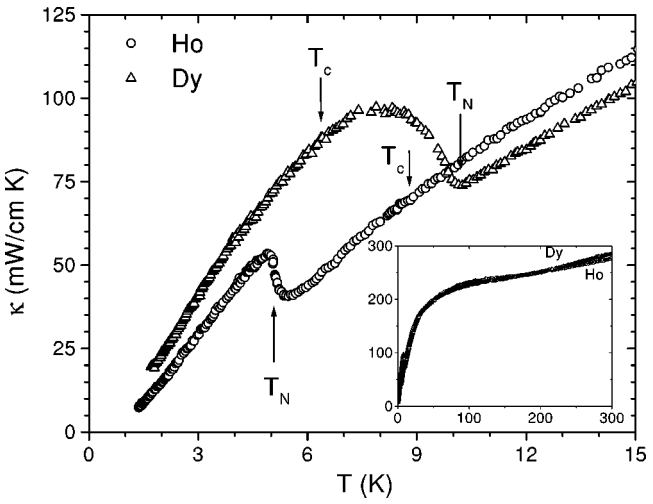

FIG. 2. κ(mW/cm K) vs $T(K)$ for $HoNi_2B_2C$–○ and $DyNi_2B_2C$–△ for two temperature ranges. Arrows show superconducting and magnetic transitions.

Figure 2 depicts an expanded plot of the a-b plane κ of $HoNi_2B_2C$ and $DyNi_2B_2C$ plotted versus temperature from 1.5 to 30 K. The superconducting phase transition for $HoNi_2B_2C$ ($T_c = 8.5$ K which is denoted by an arrow in Fig. 2) is not indicated in the κ data of Fig. 2, and the superconducting phase transition for $DyNi_2B_2C$ ($T_c = 6.2$ K which is also denoted by an arrow in Fig. 2) is also not apparent in Fig. 2.

The data of Fig. 2 exhibit an increase in κ for $HoNi_2B_2C$ of $\sim 25\%$ at T_N, presumably due to the loss of spin-flip scattering. This ordering of magnetic moments should not affect phonons due to the apparent weak phonon to magnetic moment interaction in this family of materials. This aforementioned weak interaction is based on the fact that the change of the thermal conduction due to anti-ferromagnetic ordering is entirely accounted for by the change to electron thermal conduction for the $DyNi_2B_2C$, $TbNi_2B_2C$, and $GdNi_2B_2C$ samples as discussed above. Therefore, this large change in κ below T_c seems to be due solely to electrons. This implies that the normal, i.e., uncondensed, electron density at T_N for $HoNi_2B_2C$ is significant.

This explanation is consistent with the critical-field data of $HoNi_2B_2C$,[1] which show a peak for the temperature range

between T_c and T_N that drops sharply with a deep minimum at T_N. The large electronic contribution remaining at T_N is also consistent with point contact tunneling measurements which suggested that the superconducting state in $HoNi_2B_2C$, above the Néel temperature $T_N = 5.2$ K, does not exhibit the usual gap.[8] It is interesting to note that for $HoNi_2B_2C$ the upper critical field H_{c2} again decreases by about 3 kOe at T_N (see Naugle *et al.*[1]) consistent with the $ErNi_2B_2C$ and $TmNi_2B_2C$ upper critical-field decrease. H_{c2} is again anisotropic, however H_{c2} decreases by about the same amount for the field in the *c* and in the *a* directions for $HoNi_2B_2C$.

Since κ for $HoNi_2B_2C$ is dominated by the charge carrier thermal conduction, it is therefore surprising that there is no indication at all of the superconducting transition in the κ data. It should be noted however, that this absence of an indication coupled with the dominance of κ_e for $HoNi_2B_2C$ is consistent with predictions by Ambegaokar and Griffin[9] that there should not be a clear change in the electronic thermal conductivity at the onset of gapless superconductivity.

For $HoNi_2B_2C$, κ also shows a weak feature at about $T = 5.5$ K, which agrees well with T_{M1}, one of the two other magnetic transition temperatures reported by Canfield *et al.*[10] An even weaker feature in $\kappa(T)$ can be discerned, with a good imagination, when the data around T_N is expanded at the third magnetic transition temperature at $T = 6.0$ K, T_{M2}. Neither of these are visible in Fig. 2 due to the scale of the plot.

Figure 2 depicts the thermal conductivity data for $DyNi_2B_2C$ ($T_N = 10.3$ K). Notice that κ starts to increase sharply at T_N, again presumably due to the loss of spin-flip scattering. It is noteworthy that the reduction in scattering at T_N is mostly accounted for by the reduction in the scattering of the charge carriers, as mentioned before. This implies that the magnetic phase transition has a minimal effect on phonons. Again this conclusion is based on the measured ρ and again assumes that the Wiedemann-Franz law is valid near T_c.

C. κ of $TbNi_2B_2C$ and $GdNi_2B_2C$

The inset of Fig. 3 depicts the $a-b$ plane κ of $TbNi_2B_2C$ and $GdNi_2B_2C$ plotted versus temperature from 1.5 to 300 K. The high temperature κ for both materials is again approximately linear in temperature; however, the magnitude of κ for $GdNi_2B_2C$ is uncharacteristically high as compared to the other members of the RNi_2B_2C family reported here. Using a Wiedemann-Franz analysis with the measured ρ for these two samples, κ for $TbNi_2B_2C$ is dominated by the electronic portion κ_e at T_N, while for $GdNi_2B_2C$ κ_e is about one-half of the total measured κ at T_N. At 300 K, κ_e for $TbNi_2B_2C$ is just above one-half of the total measured κ, and κ_e for $GdNi_2B_2C$ is below one-half of the total measured κ. Once again electrons appear to be responsible for roughly one-half or more of the thermal conduction for the entire temperature range from 1.5 to 300 K in these two materials. *S* and ρ for these two materials are also metallic in nature, as discussed later in this paper. Again it is noteworthy that there is no sign of a phonon or electron peak in the high temperature thermal conductivity for either $TbNi_2B_2C$ or $GdNi_2B_2$ well past the temperature of the ordinary peak, $(0.1–0.3)\Theta_D$. The Debye temperature is estimated as $\sim 354–359$ K for $TbNi_2B_2C$ and $\sim 355–360$ K for $GdNi_2B_2C$ by scaling of molar masses from $LuNi_2B_2C$.

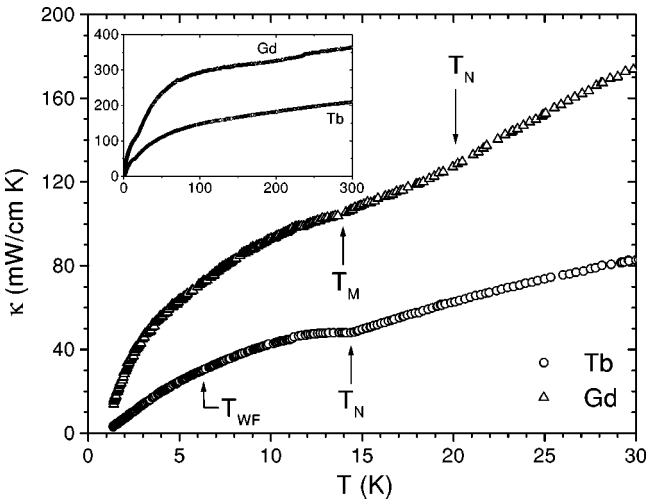

FIG. 3. κ(mW/cm K) vs $T(K)$ for $TbNi_2B_2C$–○ and $GdNi_2B_2C$–△ for two temperature ranges. Arrows show magnetic transitions.

Figure 3 depicts an expanded plot of the $a-b$ plane κ of $TbNi_2B_2C$ and $GdNi_2B_2C$ plotted versus temperature from 1.5 K to 30 K. The thermal conductivity for $TbNi_2B_2C$ ($T_N \simeq 14$ K) clearly starts to increase at T_N, although not as sharply as that for $DyNi_2B_2C$. Also, the change in κ due to the reduction in scattering at T_N is again totally accounted for by the reduction in scattering of the charge carriers, i.e., $\kappa_{total} - \kappa_e$ (not shown in Fig. 3) does not change at T_N for $TbNi_2B_2C$.

The second-order antiferromagnetic to weak ferromagnetic transition $T_{WF} = 6–8$ K, which is denoted by an arrow in Fig. 3, is not indicated in the $TbNi_2B_2C$ data of Fig. 3. This is similar to the absence of an indication of the weak ferromagnetic phase transition at T_{WF} for both $ErNi_2B_2C$ samples (see Fig. 1 and the earlier discussion). This absence of a clear indication of the weak ferromagnetic phase transition in the thermal conductivity data could be explained by the fact that this transition does not strongly affect the scattering of charge carriers. Evidence to support this possibility is the fact that an indication of this magnetic transition is only a subtle change in slope in the $TbNi_2B_2C$ electrical resistivity data, as discussed later in this paper. Additionally, this antiferromagnetic to weak ferromagnetic transition could very easily have little or no impact on phonon scattering, as appears to be the case for the paramagnetic to antiferromagnetic transition for $DyNi_2B_2C$, $TbNi_2B_2C$, and $GdNi_2B_2C$.

The thermal conductivity data for $GdNi_2B_2C$ ($T_N = 20$ K, which is denoted by an arrow in Fig. 3) show a subtle change in the slope of κ at T_N, which is less clear than that for $TbNi_2B_2C$. It is interesting that at T_N, the electronic portion of κ is only one-half of the total measured κ. This differs from all of the other members of the RNi_2B_2C family except for $YbNi_2B_2C$. This could partly explain the

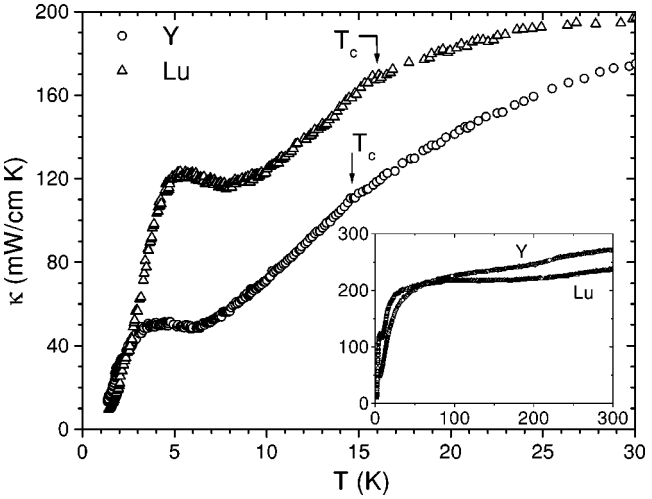

FIG. 4. κ(mW/cm K) vs T(K) for YNi_2B_2C–○ and $LuNi_2B_2C$–△ for two temperature ranges. Arrows show superconducting transitions.

lack of a clear indication in κ at T_N which is a first-order phase transition in the specific heat as reported by Hilscher and Michor.[11] $GdNi_2B_2C$ also has the highest T_N, which implies the greatest spin fluctuations due to thermal energy, of all of the members of the RNi_2B_2C which order antiferromagnetically. This could also help explain the lack of a clear indication of T_N in κ data. At the lower modulated antiferromagnetic ordering temperature $T_M = 14$ K, which is denoted by an arrow in Fig. 3, there is a subtle change in the slope of κ. Again, it is worthwhile to note that, as discussed later in this paper, this magnetic phase transition is only weakly indicated in the $GdNi_2B_2C$ resistivity data. This implies that this transition does not strongly affect the scattering of charge carriers, which could help to explain why this transition is not clearer in the κ data.

Thermal conductivity data for temperatures below 25 K were previously reported by Cao *et al.*[7] for a polycrystalline sample of $GdNi_2B_2C$. The data reported in this paper are about 500% greater in magnitude than that reported by Cao *et al.* Additionally, the data of Cao *et al.* did show an indication of T_N but do not show an indication of T_M in the polycrystalline data of $GdNi_2B_2C$.

D. κ of YNi_2B_2C and $LuNi_2B_2C$

The inset of Fig. 4 depicts the a–b plane κ of YNi_2B_2C and $LuNi_2B_2C$ plotted versus temperature from 1.5 to 300 K. The high temperature κ for both materials is approximately linear in temperature and close in magnitude. Using a Wiedemann-Franz analysis with the measured ρ for these two samples, the electronic portion κ_e is about two-thirds of the total measured κ for both YNi_2B_2C and $LuNi_2B_2C$ from T_c to 300 K. Additionally, S and ρ for these two materials are once again metallic in nature. Again it is noteworthy that there is no sign of a phonon or electron peak in the high temperature thermal conductivity for either YNi_2B_2C or $LuNi_2B_2C$ well past the temperature of the ordinary phonon peak, $(0.1–0.3\Theta_D)$. This indicates that the anomalous high-temperature behavior of κ in the rare-earth nickel borocarbides is not associated with magnetic scattering. The Debye temperature was reported as ~490 K by Movshovich *et al.*[12] or ~540 K by Hong *et al.*[13] for YNi_2B_2C, and ~350 K by Carter *et al.*[5] or ~345 K by Kim *et al.*[6] for $LuNi_2B_2C$.

Hilscher and Michor[11] reported that the magnitude of the lattice contribution to the specific heat c_{ph} of $LuNi_2B_2C$ increases by about 125% as the temperature increases from 200 to 300 K. Figure 4 shows that the magnitude of the high temperature κ of $LuNi_2B_2C$ increases by only about 10% over this same temperature interval. Taking the charge-carrier contribution κ_e to be temperature independent at these higher temperatures, the lattice contribution κ_{ph} then increases by about 30% since it is roughly one-third of the total thermal conductivity over this temperature interval. Using the simple relation $\kappa_{ph} = c_{ph} v l/3$, and taking the velocity of sound to be approximately constant over this temperature range, the phonon mean free path must decrease rather strongly ($l_{300K} \simeq 0.24\ l_{200K}$) in $LuNi_2B_2C$ over this temperature interval. The typical phonon-phonon scattering should cause the phonon mean free path to decrease as $1/T$, i.e., $l_{300K} \simeq 0.66\ l_{200K}$. This suggests that some other scattering mechanism, probably phonon-electron scattering, in addition to the typical phonon-phonon scattering is important at higher temperatures. This lends further evidence to the apparent strong electron-phonon interaction in the family of materials and particularly in $LuNi_2B_2C$.

Figure 4 depicts an expanded plot of the a-b plane κ of YNi_2B_2C and $LuNi_2B_2C$ plotted versus temperature from 1.5 K to 30 K. The superconducting phase transitions ($T_c = 15.7$ K and 16.6 K for YNi_2B_2C and $LuNi_2B_2C$, respectively) are clearly indicated in κ as a distinct change in slope as expected for a second-order phase transition. Both of the nonmagnetic superconductors YNi_2B_2C and $LuNi_2B_2C$ also clearly exhibit a strong enhancement in the low temperature κ below T_c as shown in Fig. 4. The low temperature peak for the YNi_2B_2C sample is lower in magnitude, and peaks at a lower temperature than that for the $LuNi_2B_2C$ sample. None of the magnetic superconductors (R=Tm, Er, Ho, and Dy) exhibit a similar broad enhancement in the low temperature κ.

Sera *et al.*[14] indicated that the simplest explanation for the enhancement in κ in the superconducting state is an increase in the phonon thermal conductivity due to reduced phonon-electron scattering as the normal electrons condense into Cooper pairs. This explanation is consistent with recent inelastic neutron scattering experiments for YNi_2B_2C (Ref. 15) and for $LuNi_2B_2C$,[16] which showed an anomalous phonon behavior (soft phonon modes) below T_c and suggested strong electron-phonon coupling for both these materials. These reduced energy phonon modes, one optical and one transverse acoustic,[11] lay below 2Δ, the condensation energy of a Cooper pair. This means that the phonon modes could not decay by breaking a Cooper pair, and therefore the lifetime of the soft phonon mode is increased. Additionally, the thermal conductivity measurements performed on YNi_2B_2C by Sera *et al.*[14] in an external magnetic field showed that this enhancement was easily suppressed by external fields above

the lower critical field value, lending evidence to the argument for strong electron-phonon interaction in these two materials. It should be noted that Boaknin *et al.*[17] also independently observed the enhancement for $LuNi_2B_2C$, and reported that the very low temperature behavior of κ was cubic in temperature indicating phonon heat conduction limited by boundary scattering.

A less likely explanation for the enhancement is the convective contribution to the thermal conductivity discussed by Ginzburg.[18] This convective contribution is proportional to the normal, i.e., uncondensed, charge carrier component times $(k_B T_c/E_F)^2$, where E_F is the Fermi energy. This convective contribution should be negligible for these two materials due to the low superconducting transition temperatures. Another possible explanation is that the samples become ''transparent'' to phonons as the temperature approaches that of the peak temperatures. This could be a result of the sample changing with temperature, e.g., a lattice constant tuning, the result of the dominant phonon frequency which varies with temperature, or a combination of the two.

The low-temperature enhancement in the nonmagnetic superconductors YNi_2B_2C and $LuNi_2B_2C$ is caused by an increase in the phonon conductivity. However, κ for the magnetic superconductors does not show a similar enhancement. Two conclusions of Hennings[4] could help explain this absence of an enhancement below T_c for the magnetic materials. The proportion of κ_{total} due to κ_e is much smaller for the magnetic $R=$Tm, Er, Ho, and Dy than for the nonmagnetic $R=$Y and Lu, and therefore that due to phonons is greater for the magnetic samples. Also the electron-phonon interaction seems to be weaker for the magnetic superconductors as compared to the nonmagnetic superconductors. Then the phonon heat conduction contribution at T_c starts at a higher proportion of the total κ and increases less, while κ_e starts at a lower proportion of the total thermal conductivity and decreases less which could explain the absence of an enhancement. Additionally, the phonon spectra for the magnetic superconductors is unknown and could be different from that of the magnetic superconductors.

E. Electrical resistivity

The high temperature ($T \geqslant 100$ K) ρ for all of the samples of the RNi_2B_2C family investigated here is approximately linear in temperature with varying slight amounts of curvature down toward the temperature axis. The room temperature ρ's vary from 40 to 72 $\mu\Omega$ cm. Figure 5 shows the *a*-*b* plane, direct current electrical resistivity versus temperature for the first $ErNi_2B_2C$ sample from 1.5 to 300 K. The temperature dependence of the high temperature ρ shown for this sample is typical of all of the members of the RNi_2B_2C family discussed in this paper. The residual resistivity ratios (RRR's), range from 11.9 to $\geqslant 29.7$, and the residual resistances ρ_o's are all $\leqslant 5$ $\mu\Omega$ cm. For $R=$Tm, Er, and Ho, ρ_o was taken to be $\rho(T_c+)=\rho_o'+\rho_{spd}$ where ρ_o' is the standard $(T=0)$ residual resistivity. The spin disorder resistivity, ρ_{spd}, is defined as the decrease in resistivity due to the reduction in scattering as the magnetic moments of the trivalent rare-earth ions order antiferromagnetically. The three highest ρ_o's ($R=$Tm, the first Er, and Ho) are the modified ρ_o's that include ρ_{spd}. Additionally, the three lowest RRR's ($R=$Tb, Gd, and Dy) are artificially deflated due to the exclusion of ρ_{spd} in ρ_o.

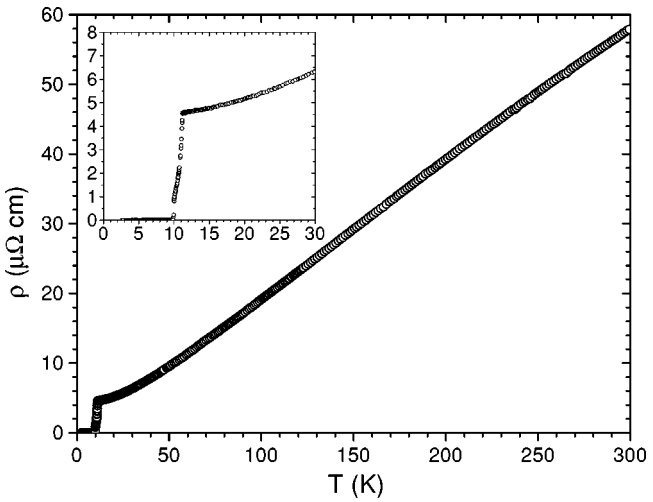

FIG. 5. $\rho(\mu\Omega\,\text{cm})$ vs T(K) for the first $ErNi_2B_2C$ sample for two temperature ranges.

The superconducting transitions are all sharp, with the exception of the first $ErNi_2B_2C$ sample, and are all complete, with the exception of the both $ErNi_2B_2C$ samples, and correspond to the T_c for the bulk material. Overall, the resistivity data shows that these are all high quality single-crystal samples, except for the first $ErNi_2B_2C$ sample which appears to be a lower quality sample and clearly has one or more unwanted phases or contaminants present.

The disordered paramagnetic to ordered antiferromagnetic transition shows up clearly for the three samples where superconductivity does not mask it ($R=$Dy, Tb, and Gd). This transition also occurs at the correct temperatures for all three, *i.e.*, at a temperature corresponding to T_N for the bulk material. The decrease in ρ below T_N shown in Fig. 6 for $DyNi_2B_2C$, $TbNi_2B_2C$, and $GdNi_2B_2C$ is due mainly to the loss of spin-disorder resistivity.[19] A sharp kink in ρ at $T=T_N$ is evidence, according to Gratz and Zuckermann,[19] that there are localized magnetic moments whose properties cannot be satisfactorily explained by a band model.

The low-temperature weak ferromagnetic transition, reported in the literature, e.g., Lynn *et al.*,[20] as occurring at $T_{WF}=6-8$ K, appears only as a subtle change in the slope of the $TbNi_2B_2C$ resistivity data of Fig. 6. The lower temperature magnetic transition for $GdNi_2B_2C$, reported in the literature, e.g., Detlefs *et al.*,[21] as occurring at $T_M=13$ K, again appears as a subtle change in slope in the $GdNi_2B_2C$ resistivity data of Fig. 6, but between 14 and 15 K. There is also a small broad feature in the ρ data between 5 and 9 K that does not correspond to any clear feature in the κ data.

Figure 6 is a plot of the low-temperature electrical resistivity versus temperature for the three compounds that have antiferromagnetic ordering that is not masked by superconductivity, $DyNi_2B_2C$, $TbNi_2B_2C$, and $GdNi_2B_2C$. The data clearly indicate that the sharpness of the change in ρ at the

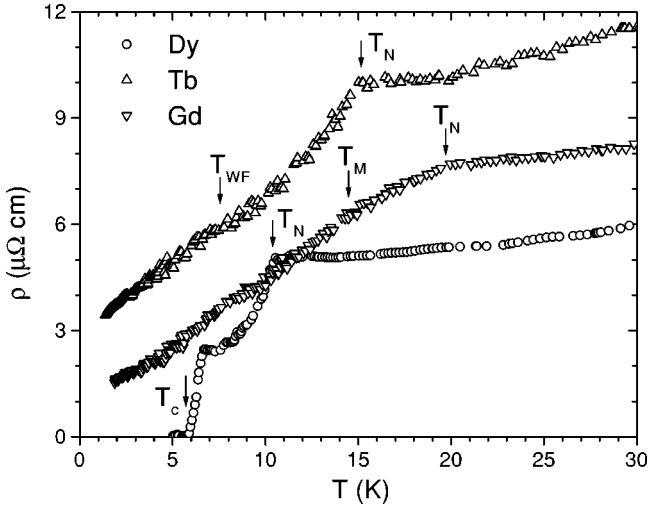

FIG. 6. $\rho(\mu\Omega$ cm) vs T (K) for $DyNi_2B_2C$–○, $TbNi_2B_2C$–△, and $GdNi_2B_2C$–▽. Arrows show superconducting and magnetic transitions.

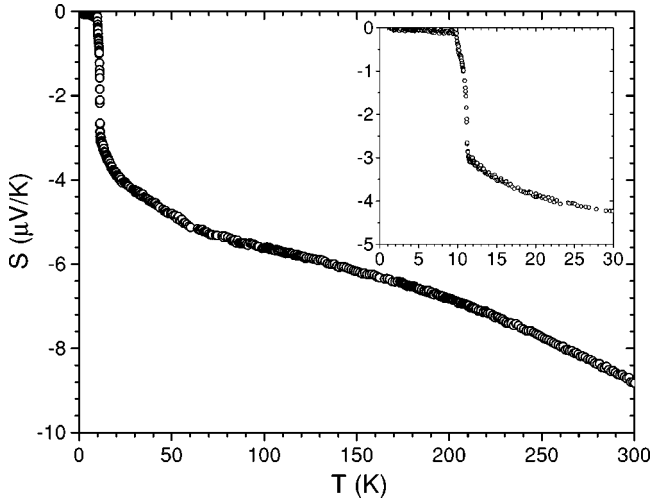

FIG. 7. $S(\mu$V/K) vs $T(K)$ for the first $ErNi_2B_2C$ sample for two temperature ranges.

ordering temperature decreases from $DyNi_2B_2C$ to $GdNi_2B_2C$. The data for $DyNi_2B_2C$ is much different than that of $TbNi_2B_2C$, and $GdNi_2B_2C$. This should be expected due to differences of the antiferromagnetic order below T_N. $DyNi_2B_2C$ goes from having disordered spins to a commensurate antiferromagnetic order, ferromagnetic sheets stacked antiferromagnetically. In contrast to this, $TbNi_2B_2C$ and $GdNi_2B_2C$ both go to a modulated incommensurate antiferromagnetic order at T_N.

Complete magnetic order exists at zero temperature, but at any non-zero temperature there will be spin fluctuations due to the thermal excitation energy, and these fluctuations will be the greatest just below T_N. These spin fluctuations will certainly reduce the effect of ordering in decreasing the electrical resistivity at T_N. Since T_N increases from about $T_N=10.3$ K for $DyNi_2B_2C$ through $T_N=14$ K for $TbNi_2B_2C$ to $T_N=20$ K for $GdNi_2B_2C$, it is natural to expect the resistivity transition to be the least sharp for $GdNi_2B_2C$ and the sharpest for $DyNi_2B_2C$ just as the data of Fig. 6 show. Additionally, the phonon scattering at T_N is greater for the higher T_N values and is a higher percentage of the total scattering, which means the decrease in spin flip scattering will be relatively less important for higher T_N values.

F. Thermoelectric power

The absolute thermoelectric power of all the compounds discussed in this paper is similar in temperature dependence and close in magnitude to that reported previously by Rathnayaka *et al.*[22] and Bhatnagar *et al.*[23] for other single-crystal samples of these materials. The high temperature ($T \geqslant 100$ K) S for $R=$ Y and Lu-Dy is approximately linear in temperature dependence and is negative for the entire temperature range. Each of these materials also has a quite large (negative 2–6 μV/K) intercept when the linear portion is extrapolated down to T $=0$ K. This behavior in S is quite anomalous as discussed earlier,[22,23] as is the high temperature thermal conductivity. The room temperature S's range from 7 to 14 μV/K. Figure 7 shows the a-b plane absolute thermopower versus temperature for the first $ErNi_2B_2C$ sample from 1.5 to 300 K. The temperature dependence of the high temperature S shown for this sample is typical of all of the members of the RNi_2B_2C family discussed in this paper, except for $R=$ Tb and Gd. An analysis of the thermoelectric power (see Hennings[4] for detailed discussion) that was somewhat similar to that performed earlier by Bhatnagar *et al.*,[23] indicates that the presence of disordered magnetic spins adds a term linear in temperature and proportional to the de Gennes factor of the trivalent rare-earth ions to the high-temperature thermoelectric power. This conclusion is in agreement with the general results reported earlier by Gratz and Zuckermann[19] for rare-earth transition-metal compounds.

The thermoelectric power below the magnetic ordering temperature of $DyNi_2B_2C$, $TbNi_2B_2C$, and $GdNi_2B_2C$ in Fig. 8 all show a low-temperature enhancement in the mag-

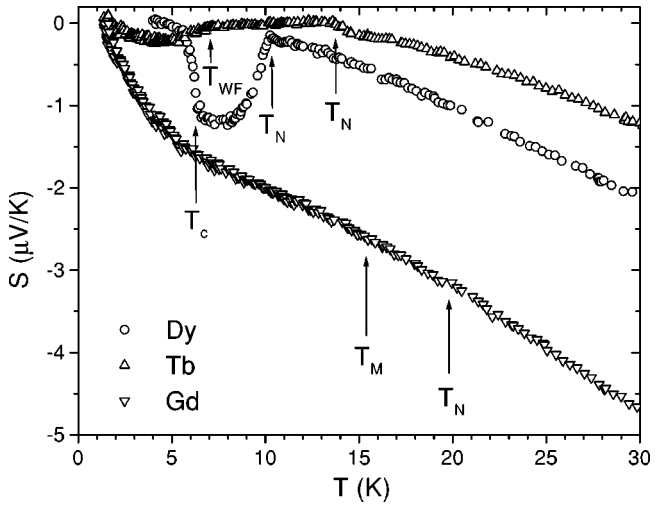

FIG. 8. $S(\mu$V/K) vs T(K) for $DyNi_2B_2C$–○, $TbNi_2B_2C$–△, and $GdNi_2B_2C$–▽. Arrows show superconducting and magnetic transitions.

nitude of S above that of the paramagnetic state. For all three materials, this enhancement occurs at temperatures below T_N. For $DyNi_2B_2C$ ($T_N = 10.3$ K), the enhancement in the magnitude of S is the greatest of the three, starts sharply at T_N, peaks at about $T = 8$ K, and is driven down to zero at the onset of superconductivity at $T_c = 6.2$ K. For $TbNi_2B_2C$ ($T_N = 14$ K), there is a sharp change in the slope of S at T_N. The magnitude of S increases slowly with decreasing temperature until about $T_{WF} = 7$ K. At T_{WF} there is another change in the slope of S and the magnitude of S increases much more quickly until it begins to decrease below about $T = 4$ K. For $GdNi_2B_2C$ ($T_N = 20$ K), there is a very subtle change in the slope of S at T_N which is denoted by an arrow in Fig. 8. At the lower modulated antiferromagnetic ordering temperature $T_M = 14$ K, which is denoted by an arrow in Fig. 8, there is a second subtle change in the slope of S, below which the magnitude of S is enhanced until it decreases rapidly below about $T = 5$ K. There is also a subtle feature in the S data corresponding to the small, broad feature in ρ between 5 and 9 K.

One possible cause of this low temperature magnetic ordering enhancement in the magnitude of S is a contribution within the diffusion thermoelectric power, $S_d(T)$. This contribution could result from the reduction in scattering at T_N due to the loss of spin-flip scattering for all three materials as the rare-earth magnetic moments order antiferromagnetically. This reduction in scattering is clearly seen in plots of the electrical resistivity versus temperature, (Fig. 6), for $DyNi_2B_2C$, $TbNi_2B_2C$, and $GdNi_2B_2C$. The resistivity exhibits the sharpest and greatest decrease in scattering at T_N for $DyNi_2B_2C$, and the smallest and least sharp decrease for $GdNi_2B_2C$. This is analogous to the sharpness and magnitude of the enhancement of S for these three materials. Note that in S it is $\partial\tau/\partial\epsilon$ that must change, not τ as in ρ and κ. Since spin-flip scattering is completely lost at T_N, its contribution to $\partial\tau/\partial\epsilon$ is also lost, and this will be reflected in the total $\partial\tau/\partial\epsilon$. Therefore, as long as $\partial\tau/\partial\epsilon$ for magnetic scattering is nonzero, there should be a change in S at T_N. Also note that the resistivity of $TbNi_2B_2C$ shows a subtle indication of T_{WF}, whereas the low-temperature enhancement in the magnitude of S begins quite sharply for $TbNi_2B_2C$ at T_{WF}.

A second possible cause of this low temperature magnetic ordering enhancement in the magnitude of S is a contribution to the thermoelectric power, $S_m(T)$, which is due to the presence of magnetism and or magnetic ions within the samples. This contribution could result from a magnon drag effect due to the electron-magnon interaction. This explanation seems reasonable for $DyNi_2B_2C$, $TbNi_2B_2C$, and $GdNi_2B_2C$, given the ordered magnetic states of these materials and low temperatures of the enhancement. The enhancement occurs at temperatures of $T = 10.3$ K for $DyNi_2B_2C$, $T = 7$ K for $TbNi_2B_2C$, and $T = 14$ K for $GdNi_2B_2C$. These temperatures may seem to be slightly high for magnons to be important, but Blatt *et al.*[24] attributed the large peak in the thermoelectric power of ferromagnetic iron at 200 K to magnon drag effects. Additionally, for magnon drag to be important in S, magnons would also be expected to contribute appreciably to the thermal conduction.

G. Quality of the $ErNi_2B_2C$ samples

The inset of Fig. 5 is an expanded view of the low temperature $a-b$ plane resistivity versus temperature for the first $ErNi_2B_2C$ sample. The low temperature ρ data for $ErNi_2B_2C$ sample number one show the onset of superconductivity at 11.2 K which agrees well with that of the highest quality single-crystal samples. The superconducting transition is not sharp with a slight ''shoulder'' at low values of resistivity. Additionally, the superconducting phase transition is not complete until about $T = 5.5$ K (not visible on the inset of Fig. 5 due to scale) indicating that this may not be a single phase single crystal sample. The residual resistivity ratio $\rho(300\text{ K})/(\rho_o' + \rho_{spd})$, where $(\rho_o' + \rho_{spd}) = \rho(T_c+)$, for $ErNi_2B_2C$ sample number one is 12.7. The spin disorder resistivity ρ_{spd} is defined as the decrease in resistivity at T_N. Additionally, $\rho(T_c+)$ for this sample is 4.5 $\mu\Omega$ cm. The inset of Fig. 7 is an expanded view of the low temperature $a-b$ plane thermopower versus temperature for the first $ErNi_2B_2C$ sample. The S data for $ErNi_2B_2C$ sample number one show the onset of superconductivity at 11.2 K, a ''shoulder,'' and completion of the phase transition at around $T = 5$ K which agrees exactly with the superconducting transition depicted in the resistivity data.

The first $ErNi_2B_2C$ sample has the highest ρ_o of all of the materials investigated here, one of the lower RRR's of all of the materials investigated here, and the ''shoulder'' in the superconducting transition of both ρ and S, neither of which go to zero until around $T = 6$ K. All of these facts suggest that this sample may not be totally a single crystal, or may have an unwanted phase (non–1221) present. It is also possible that the first $ErNi_2B_2C$ sample may be contaminated with a different rare-earth. $DyNi_2B_2C$ is a great candidate for the contaminant since T_c is 6.2 K and the ρ and S data go to zero around 6 K. Additionally, T_N for $DyNi_2B_2C$ is 10.3 K and the ''shoulder'' in the ρ and S superconducting transitions for $ErNi_2B_2C$ is just above 10 K.

The low temperature ρ data for $ErNi_2B_2C$ sample number two contain a very sharp superconducting transition without the ''shoulder'' contained in the ρ data of the first $ErNi_2B_2C$ sample, but the phase transition is again not complete until about $T = 5.5$ K. The remaining resistance between 5.5 and 11 K is a slightly greater percentage of the value at T_c+ than that for the first $ErNi_2B_2C$ sample. The RRR for the second $ErNi_2B_2C$ sample is 14.3. The S data for the second $ErNi_2B_2C$ sample show a very sharp superconducting transition that drops to zero at about $T = 11$ K. The absence of a ''shoulder'' and the sharpness of the transition are similar to the resistance data for this sample. Based on this and the higher RRR, the second $ErNi_2B_2C$ sample was determined to be of higher quality than the first $ErNi_2B_2C$ sample. The S data for the second $ErNi_2B_2C$ sample indicate that the transition is complete at about 11 K, unlike the resistance data for this sample and unlike both the ρ and S data for the first $ErNi_2B_2C$ sample. The magnitude of S for the second $ErNi_2B_2C$ sample is slightly lower than that of the first

$ErNi_2B_2C$ sample. All of these facts suggest that the second $ErNi_2B_2C$ sample is a higher-quality single crystal than the first $ErNi_2B_2C$ sample even though the superconducting transition is again not complete at 11 K.

One possible cause of this ''step'' in the low temperature ρ (below T_c) of both $ErNi_2B_2C$ samples could be related to the silver epoxy used to attach the two voltage leads to the samples for the four-terminal ρ measurements. This is an unlikely cause considering that ρ's of the other eight RNi_2B_2C samples (five of whom are superconducting in this temperature range) were measured with the same method and none of them show a similar ''step.'' A second possible cause of this ''step'' could be a material property specific to $ErNi_2B_2C$. Examples of this would be unconventional gap behavior or perhaps an uncharacteristically low critical current density. The electrical current used for ρ measurement varied from sample to sample, but was the lowest current (1, 3, or 5 mA) that gave an acceptable signal to noise ratio. The first and second $ErNi_2B_2C$ samples had the fourth smallest and smallest, respectively, cross-sectional areas of the ten samples investigated.

IV. CONCLUSIONS

The high temperature thermal conductivities of all of the single-crystal rare-earth nickel borocarbides discussed by this paper are approximately linear in temperature, and the electronic heat conduction contributes more than half, except for $GdNi_2B_2C$, where the charge carriers are responsible for just less than one-half of the total thermal conductivity. These results assume that the Wiedemann-Franz law is applicable, i.e., inelastic scattering is not dominant. All of these materials are metalliclike based on S and ρ. The high temperature behavior of the thermal conductivity for all of these metalliclike compounds is anomalous. This anomaly is the absence of a peak around $0.1–0.3\ \Theta_D$, and a consequent increase of κ with temperature.

The thermal conductivities well below T_c of YNi_2B_2C and $LuNi_2B_2C$ are both clearly dominated by phonon conduction as indicated by the enhancement in thermal conductivity. The failure of Wiedemann-Franz law in the temperature range of $T=20\ \mathrm{K}–80\ \mathrm{K}$ for both YNi_2B_2C and $LuNi_2B_2C$, which was discussed in detail by Hennings,[4] means that inelastic scattering is very important at these temperatures and that suggests that electron-phonon scattering is dominant. All of this is evidence supporting a strong electron-phonon coupling for both of these materials. Based on the behavior of κ, S, and ρ, the strength of the electron-phonon coupling seems to decrease across this family from the non-magnetic $LuNi_2B_2C$ to the magnetic $GdNi_2B_2C$. This result is consistent with the conclusions of Gratz and Zuckermann,[19] for their studies of many families of rare-earth transition metal compounds.

The magnetic moment-phonon interaction is very weak at best, and possibly nonexistent. This result is based on the behavior of the electrical resistivity and thermal conductivity at the magnetic ordering temperatures and the fact that the phonon heat conduction does not change at T_N. The presence of disordered magnetic spins has been found to add a term linear in temperature and proportional to the de Gennes factor to the high temperature thermo-electric power consistent with the work of others.[1,19,23] There is also a low temperature enhancement in the magnitude of the thermoelectric power that is not masked by superconductivity for the three samples that have antiferromagnetic order above T_c. The magnetic moments are responsible for interesting effects in the low-temperature thermal conductivity such as the gapless superconductivity in $HoNi_2B_2C$. The sharp increase in the thermal conductivity of $TmNi_2B_2C$ at $T=1.4$ K is probably due to additional heat conduction by magnons. Future measurements below $T=1.4$ K could better delineate the nature of this effect.

Finally, the results for the two $ErNi_2B_2C$ samples indicate the strong dependence of the thermal conductivity on the quality of the single-crystal sample. This indicates that even though the electron thermal conduction dominates, the lattice contribution to the thermal conductivity is important.

ACKNOWLEDGMENTS

This work was supported by the Texas Center for Superconductivity and Advanced Materials at the University of Houston (TCSAM), the Robert A. Welch Foundation (A-0514), and the NSF (DMR-0111682 and 0103455). Ames Laboratory is operated for the U.S. DOE Office of Basic Energy Services by ISU under Contract No. W-7405-Eng-82.

*Electronic address: bhennings@lynntech.com
†Electronic address: naugle@physics.tamu.edu

[1] D. G. Naugle, K. D. D. Rathnayaka, and A. K. Bhatnagar in *Studies of High Temperature Superconductors*, edited by A. Narlikar (Nova, New York, 1999), Vol. 28, p. 189.
[2] M. Xu, P. C. Canfield, J. E. Ostenson, D. K. Finnemore, B. K. Cho, Z. R. Wang, and D. C. Johnston, Physica C **36**, 91 (1977).
[3] R. B. Roberts, Philos. Mag. **36**, 91 (1977).
[4] B. D. Hennings, Ph.D. thesis, Texas A&M University, 2002.
[5] S. A. Carter, B. Batlogg, R. J. Cava, J. J. Krajewksi, W. F. Peck Jr., and H. Takagi, Phys. Rev. B **50**, 4216 (1994).
[6] J. S. Kim, W. W. Kim, and G. R. Stewart, Phys. Rev. B **50**, 3485 (1994).
[7] S. Cao, S, Sakai, K. Nishimura, and K. Mori, Physica C **341-348**, 751 (2000).
[8] L. F. Rybaltchenko, I. K. Yanson, A. G. M. Janson, P. Mandal, P. Wyder, C. Tomy, and D. McK. Paul, Physica B **218**, 189 (1996).
[9] V. Ambegaokar and A. Griffin, Phys. Rev. **137**, A1151 (1965).
[10] P. C. Canfield, B. K. Cho, D. C. Johnston, D. K. Finnemore, and M. F. Hundley, Physica C **230**, 397 (1994).
[11] G. Hilscher and H. Michor in *Studies of High Temperature Superconductors* (Ref. 1), p. 241.
[12] R. Movshovich, M. F. Hundley, J. D. Thompson, P. C. Canfield, B. K. Cho, and A. V. Chubukov, Physica C **227**, 381 (1994).
[13] N. M. Hong, H. Michor, M. Vybornov, T. Holubar, P. Hundegger, W. Perthold, G. Hilscher, and P. Rogl, Physica C **227**, 85 (1994).
[14] M. Sera, S. Kobayash, M. Hiroi, N. Kobayashi, H. Takeya, and K. Kadowaki, Phys. Rev. B **54**, 3062 (1996).

[15] H. Kawano, H. Yoshizawa, H. Takeya, and K. Kadowaki, Phys. Rev. Lett. **77**, 4628 (1995).
[16] P. Dervenagas, M. Bullock, J. Zaretsky, P. C. Canfield, B. K. Cho, B. Harmon, A. I. Goldman, and C. Stassis, Phys. Rev. B **52**, 9839 (1995).
[17] E. Boaknin, R. W. Hill, C. Lupien, L. Taillefer, and P. C. Canfield, Physica C **341-348**, 1845 (2000).
[18] V. L. Ginzburg, Usp. Fiz. Nauk. **168**, 363 (1998). [Phys. Usp. **41**, 307 (1998)].
[19] E. Gratz and M. J. Zuckermann, in *Handbook on the Physics and Chemistry of Rare Earths*, edited by K. A. Gschneidner Jr and L. Eyring (North-Holland, Amsterdam, 1982), Chap. 42, p. 117.
[20] J. W. Lynn, S. Skanthakumar, Q. Huang, S. K. Sinha, Z. Hossain, L. C. Gupta, R. Nagarajan, and C. Godart, Phys. Rev. B **55**, 6584 (1997).
[21] C. Detlefs, A. I. Goldman, C. Stassis, P. C. Canfield, S. L. Bud'ko, J. P. Hill, and D. Gibbs, Phys. Rev. B **53**, 6355 (1996).
[22] K. D. D. Rathnayaka, A. K. Bhatnagar, A. Parasiris, D. G. Naugle, P. C. Canfield, and B. K. Cho, Phys. Rev. B **55**, 8506 (1997).
[23] A. K. Bhatnagar, K. D. D. Rathnayaka, D. G. Naugle, and P. C. Canfield, Phys. Rev. B **56**, 437 (1997).
[24] F. J. Blatt, D. J. Flood, V. Rowe, P. A. Schroeder, and J. E. Coix, Phys. Rev. Lett. **18**, 395 (1967).